Hindawi
International Journal of Polymer Science
Volume 2021, Article ID 6642112, 15 pages
https://doi.org/10.1155/2021/6642112

Research Article

Preparation of Biocomposite Material with Superhydrophobic Surface by Reinforcing Waste Polypropylene with Sisal (*Agave sisalana*) Fibers

Seyoum Getaneh Abebayehu[1] **and Adam Mekonnen Engida**[1,2]

[1]*Department of Industrial Chemistry, Addis Ababa Science and Technology University, Addis Ababa, Ethiopia*
[2]*Nanotechnology Center of Excellence, Addis Ababa Science and Technology University, Addis Ababa, Ethiopia*

Correspondence should be addressed to Adam Mekonnen Engida; adam.mekonnen@aastu.edu.et

Received 27 November 2020; Revised 1 January 2021; Accepted 12 January 2021; Published 5 February 2021

Academic Editor: Hossein Roghani-Mamaqani

Nowadays, eco-friendly, renewable, and biodegradable biocomposites are among the most intensely sought materials of choice. Biocomposites have been widely used as substitutes for plastics due to their biodegradability. However, biocomposite materials absorb water and ultimately loss mechanical properties that affect service life. In this work, a biocomposite material with superhydrophobic surface was prepared by reinforcing waste polypropylene with sisal (*Agave sisalana*) fibers. The biocomposite was prepared by mixing waste polypropylene and sisal fiber with 5%, 10%, 15%, and 20% fiber loading. Based on characterization results, the composite with 15% fiber content is considered as optimum ratio. Physicochemical properties of composites were evaluated using standard American Society of Testing Materials including biodegradability test and chemical resistance test. The biodegradability of the composite before surface modification was determined by calculating weight loss and found to be 0.11%, 4.62%, 7.15%, and 10.97% for 0%, 5%, 10%, and 15% fiber loadings, and their tensile strength was 10.25 ± 0.05, 14.47 ± 0.02, 14.48 ± 0.02, and 19.90 ± 0.09 MPa for 0%, 5%, 10%, and 15% fiber content, respectively. The surface of the composite was modified for hydrophobicity by etching the surface with chromic acid followed by treating with stearic acid. The FTIR and the SEM images of unmodified and modified (superhydrophobic) surface of composites clearly state the significant difference in chemical composition and surface structure, respectively. The superhydrophobicity of the surface-modified biocomposite was defined by its self-cleaning and low wet ability properties.

1. Introduction

Plastic materials have been explored and advocated to serve as wood substituent among the various synthetic materials. They are for different applications, starting from daily use materials to complicated engineering structures and industrial applications. However, these materials are nonbiodegradable, expensive, and derived from nonrenewable resources, and they are made up of toxic substances including monomer residues, plasticizers, coloring agents, and flame retardants. On the other hand, the high resistance of polymeric materials against photo and biodegradation creates problems in regard to their accumulation and persistence in the environment [1, 2]. The most common polymers that can be used as matrix are polyethylene, polystyrene, polyvinylchloride, polylactides, and polypropylene. Among these types of plastics, polypropylene and polyethylene are widely available and used in many industrial products and household goods [3]. In order to minimize environmental burden, recycling of plastic wastes by reinforcing with natural fibers can be considered as an important means [4]. Biocomposite materials often mimic the structure of the natural fibers involved in the process and keep the strengthening properties of the matrix that is used. They represent a class of materials that can be easily processed and suited to a wide range of applications, such as packaging, building (roof structure, bridge,

window, door, and green kitchen), automobiles, aerospace, military applications, consumer products, and medical artifacts [3].

Natural fibers that are used as reinforcement are derived from biological origins which renewable source, cheap, and easily available. The other advantage of natural fiber is their low density, higher tensile strength, and stiffness than glass fibers, besides its lower manufacturing costs [5]. Natural fiber composites are very cost-effective, especially in constructions, packaging, automobile, and railway coach interiors and storage devices. Natural fiber has a hollow structure, which gives insulation against noise and heat. Because of all these, natural fiber can be a potential candidate for replacement of high-cost glass fiber for low load-bearing applications. Sisal fibers are used in different applications such as making ropes, handicrafts, papers, and textile fibers [6]. In addition to this, sisal fibers also exhibit the potential to be used as reinforcing material in commercial polymer composites due to their high strength and abundant availability. The polymer matrix is important to protect the fibers from environmental degradation and mechanical damage, to hold the fibers together and to transfer the loads on it. In polyethylene composite, it helps to improve the mechanical properties such as tensile strength, tensile modulus, and flexural strength [7]. Kebede [8] and Hung et al. [9] prepared composites for interior automobile accessories by using natural fiber (sisal fiber) as reinforcement. Similarly, Gerezgiher et al. [10] developed sisal fiber-reinforced waste polypropylene composite materials for internal door trim application and investigated the chemical resistance and flammability property of sisal fiber-reinforced waste polypropylene composite.

The major limiting factors for large-scale production of natural fiber composites are the incompatibility of natural fiber with polymer matrix and high moisture absorption. This arises from the incompatibility between the hydrophilic hydroxyl group of natural fiber and the hydrophobic polymer matrix. This leads to decreasing in mechanical and thermal properties such as tensile strength, flexural strength, and thermal stability. However, this can be improved by modifying the surface of cellulose fibers through physical and chemical methods [11]. When cellulose fibers are treated chemically or physically, its compatibility increases due to the reduction of hydroxyl group on fibers; as a result, composites' mechanical strength increases [3, 12]. High moisture absorption property of natural fiber composites is one of the major limitations in the area. Water absorption leads to swelling of the fiber, formation of voids and microcracks at the fiber matrix interface region and natural fibers create hollow structures that can hold water once it comes in contact with it. Finally, it reduces the mechanical properties and dimensional stability of composites.

This study is designed to prepare a biocomposite material with superhydrophobic to reduce water absorbing property of biocomposites. Before the preparation of the composite material, sisal fiber was treated with different concentration of 10% NaOH at specified conditions to improve its compatibility with the matrix (polypropylene). The physical and chemical properties of the composite material (with different proportion of matrix and fiber) and the sisal fiber (untreated and treated) were studied using different analytical instruments. Finally, the characterization results revealed the preparation of the biocomposite material with superhydrophobic surface. This was demonstrated by its self-cleaning and zero wettability properties which are the characteristics of superhydrophobic surface.

2. Methods and Materials

2.1. Collection of the Plant Material and Polymer Matrix. The leaf of sisal was collected from Addis Ababa Science and Technology University, Addis Ababa, Ethiopia, by cutting at their bases. The fibers were extracted manually with knife as follows: first, the leaves were cut at the base and split into strips for ease of fiber extraction. Then, the leaf was clamped between the ceramic stone and knife and was hand-pulled through in longitudinal direction gently to remove the resinous material. Finally, the extracted fiber was washed with pure water in order to remove the reaming residuals from the fibers, and then, the extracted fiber was air dried and collected for further experiments. The recycled polypropylene matrix was collected from E.K.T waste plastic recycling plant Addis Ababa, Ethiopia.

2.2. Preparation of Sisal Fiber and Cellulose Extraction. The fibers were cut into ~5-6 mm using a scissor as of Hung et al. [9], Favaro et al. [12], and Venkateshwaran et al. [13]. Then, it was washed with distilled water followed by drying for 7 days in open air. The dried fibers were treated with 10% (*w*/*v*) sodium hydroxide solution for 2 h at 90°C with stirring speeds of 200 rpm to remove the hemicelluloses and surface impurities. After the reaction time, the resulting mixture was filtered, and solid residue was washed with acetic acid to neutralize the remaining NaOH. Then, the fiber was retreated with hydrogen peroxide to remove lignin and other compounds remained on fibers. Finally, the treated cellulose fiber (CFs) was finally dried in an oven at 105°C for 24 h for further experiments.

2.3. Determination of Chemical Composition of Sisal Fiber (Untreated and Alkali Treated). The chemical composition of sisal fibers depends on the sisal varieties, producing area, and maturity of the plant. The chemical composition (cellulose, hemicelluloses, and lignin) of untreated and alkali-treated sisal fibers was determined by the method proposed by Gerezgiher et al. [10] and Mansora et al. [14].

2.3.1. Determination of the Amount of Extractives in Sisal Fiber (Untreated and Alkali Treated). The amount of extractives in sisal fiber was determined by adding 60 mL of acetone to 1 g chopped sisal fiber (*A*). The temperature was controlled at 90°C by using water bath for 2 h. After 2 h, the sample was dried in an oven at 105–110°C until constant weight was obtained (*B*). The amount of extractives was calculated by using a simple formula shown in Equation (1).

$$\text{Amount of extractive(g)} = A - B. \quad (1)$$

2.3.2. Determination of the Amount of Hemicelluloses in Sisal Fiber (Untreated and Alkali Treated). The hemicelluloses

content was determined as follows: 150 mL of 0.5 M NaOH solution was added to 1 g acetone treated and dried sample (B) (untreated and alkali treated), and the mixture was heated at controlled temperature of 80°C for 3.5 h in water bath. Next, the sample was washed with de-ionized water to remove Na^+. Then, the sample was dried in an oven at 105–110°C until constant weight was obtained (C). The amount of hemicellulose was determined by Equation (2).

$$\text{Amount of hemicelluloses(g)} = B - C. \quad (2)$$

2.3.3. Determination of the Amount of Lignin in Sisal Fiber (Untreated and Alkali Treated). The amount of lignin in sisal fiber (untreated and alkali treated) was determined by adding 30 mL of 98% sulphuric acid to 1 g acetone treated and dried sisal fiber sample (B) (untreated and alkali treated). Then, sample was left at ambient temperature for 24 h followed by heating to boiling at controlled temperature of 100°C for 1 h on heating mantel. After that, the mixture was filtered, and the solid residue was washed by using de-ionized water until sulfate ion is undetectable. Sulfate ion was determined via titration process with 10% of barium chloride solution. A white precipitate of barium sulfate would be formed if sulfate ions are present. Finally, the sample was dried in an oven at 105°C until constant weight was obtained (D). The final weight of residue is recorded as lignin content.

$$\text{Amount of lignin(g)} = D. \quad (3)$$

2.3.4. Determination of Cellulose in Sisal Fiber (Untreated and Alkali Treated). The amount of cellulose in sisal fiber (untreated and alkali treated) was determined by calculating the difference between the initial weight of the sample and the three calculated experimental components (extractive, hemicellulose, and lignin). The content of cellulose (E) was calculated from 1 g of sample by Equation (4).

$$(A - B) + (B - C) + D + E = \text{extractive} + \text{lignin} + \text{hemicellulose} + \text{cellulose} = 1\text{g}). \quad (4)$$

2.4. Composite Preparation. The fiber content and treatment of fiber with sodium hydroxide affects the water absorption capacities and chemical and mechanical properties of the composite. To see these effect, various amounts of treated and untreated sisal fiber (0, 5, 10, 15, and 20 wt%) were blended with recycled polypropylene matrix in an injection molding extruder (Thermo Forming Center 911) at 200°C for 15 min. After the plastic was melted and mixed well with the fiber for 15 min, injection molding extrusion was applied for 10 min to mold the composite materials. The NaOH treatment and content of fiber loading were the two important factors considered while preparing the composite. Finally, the composites were dried in air at room temperature and got ready for testing.

2.4.1. Composite Surface Modification. The surface of the composite was etched using chromic acid ($K_2Cr_2O_7$: H_2O : H_2SO_4; 10 : 20 : 180% w/w ratio) to create surface roughness and to introduce new polar groups as reported previously [15]. After that, 75 mg stearic acid was added into a weighing bottle containing 20 mL of water. The bottle was then put into a water bath kettle at 75°C for 15 min to dissolve the stearic acid. Afterwards, 0.5 mL of 0.3 M HCl was added into the bottle, and then, the composite was immersed into the solution for 90 min. Then samples were immediately rinsed with ethanol and dried under heat airflow at a temperature of about 70°C for 10 s.

2.5. Surface Characterization. Sisal fiber (untreated and treated) and PP/CF composites were studied using scanning electron microscope (SEM) (Inspect F50, FEI) to evaluate their surface structures. Fourier transform infrared (FTIR) spectroscopy (PerkinElmer Spectrum ES) is extensively used to evaluate surface chemistry of sisal fiber (untreated and treated) and the composites.

2.6. Biodegradation Test of the Composites with Different Fiber Content. The biodegradability of composites in soil was determined based on % weight difference of each composite before and after the experiment. The biocomposite samples with 0, 5, 10, and 15% fiber loading were cut in equal size, and their weight was accurately noted, and samples were buried in soil for 90 days. Then, the samples were collected and washed thoroughly with distilled water and allowed to dry at 105°C for 24 h. The percentage of weight loss of the specimens (Wloss) was calculated using Equation (5), the specimen weights before (W_{before}) and after (W_{after}) biodegradation according to [3].

$$W\text{loss}(\%) = \frac{W\text{before} - W\text{after}}{W\text{before}} \times 100. \quad (5)$$

2.7. Tensile Strength and Elongation. Before running the test, the specimens were formed in such a way as to form a dumbbell specimen in reference to ASTM D 638. Seven specimens of composites with 0, 5, 10, and 15% fiber loading were prepared for testing.

2.8. Chemical Resistance Test. The chemical resistance of composites was tested against sodium hydroxide, hydrochloric acid, and sulphuric acid following ASTM D 543 testing procedures [9].

$$\text{WL}(\%) = \frac{W1 - W2}{W1} \times 100, \quad (6)$$

where WL (%) is the percentage weight loss during the immersion/test period, $W1$ is weight of the specimen before immersion, and $W2$ is the weight of the specimen after the test period.

2.9. Wet Ability and Self-Cleaning Property of Modified and Unmodified Composite Material. Surface wet ability and self-cleaning of the prepared biocomposites, before and after surface modification, were determined by dropping water on surface of composites using micropipette. The observed water droplets on unmodified and modified surface were

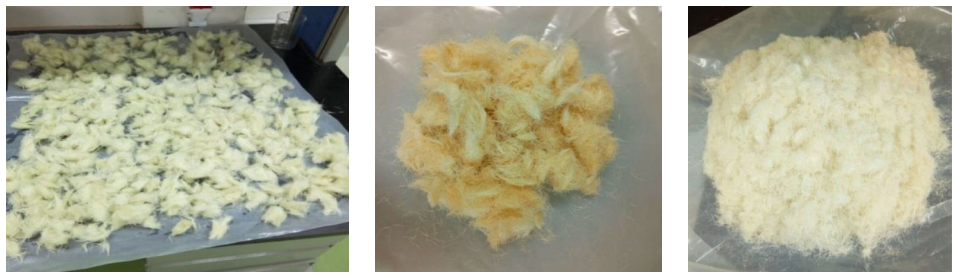

(a) (b) (c)

Figure 1: Sisal fiber (a) treated with NaOH, (b) treated with NaOH and neutralized with acetic acid, and (c) treated with NaOH and neutralized with acetic and bleached by H_2O_2.

evaluated, and images were captured. Self-cleaning properties of unmodified and modified composite surfaces were also tested by rolling water on contaminated surfaces and by dropping dirt water on surfaces.

2.10. Water Absorption Test. The water absorption capabilities of the pure PP, the PP/CFs composites, and the surface-modified PP/CF composite was tested as follows: rectangular samples were cut and then dried at 105°C in an oven until the weight remained unchanged, then cooled to room temperature in a desiccator, and their weight was determined. To investigate the percentage of absorbed water by the composites, the dried sample was immersed in distilled water for 144 hrs at room temperature by taking the weight gain at the intervals of 24 hrs. In every 24 hrs, the samples were taken, and their surface was wiped using a soft cloth, and their weight was noted sequentially. The percentage of water absorbed (W%) of the samples was calculated as shown in Equation (7):

$$(\text{wt}\%) = \frac{W2 - W1}{W1} \times 100, \quad (7)$$

where W is the percentage of water absorbed of the samples $W1$ is weight of the specimen before immersion, and $W2$ is weight of the specimen after immersion.

3. Results and Discussion

3.1. Alkali Treatment of Sisal Fiber. Modifying the surface of natural fiber improves fiber-matrix compatibility. Hence, surface modification of natural fibers is carried out to improve the interfacial adhesion between the fiber and the polymer matrix [16]. Here, the sisal fiber was treated with NaOH and H_2O_2 solution to remove lignin, hemicellulose, and other compounds. Alkali treatment using 10% NaOH was employed to enhance the adhesion property of sisal fiber with matrix and to improve the mechanical behavior of composites [17]. The alkali-treated fiber (Figure 1(a)) was neutralized with acetic acid resulting yellowish color as shown in Figure 1(b). Yellow color indicates the presence of lignin and flavones in natural fiber which is removed during further treatment of the fiber with H_2O_2 (Figure 1(c)). Hydrogen peroxides liberate per-hydroxyl ion (HOO^-) in aqueous medium. The per-hydroxyl is very unstable and reacts with oxidizable substance in fibers and cause decomposition of coloring compounds and bleaching of fibers. The whitening of the sisal fiber indicates the removal of lignin, hemicellulose, wax, and other coloring compounds which were remained on the fiber surface.

Table 1: Chemical composition of sisal fibers (untreated and treated).

Chemical	Composition (%) Untreated sisal fibers (USF)	Composition (%) Treated sisal fibers (TSF)
Extractive	6.50 ± 0.15	2.50 ± 0.23
Hemicelluloses	41.14 ± 1.140	14.50 ± 0.50
Lignin	10.40 ± 1.32	13.1 ± 2.26
Cellulose	41.96 ± 1.82	70.20 ± 4.77

3.2. Chemical Composition of Sisal Fiber (Untreated and Alkali Treated). The chemical composition of untreated and chemically treated sisal fibers was determined, and the results are summarized in Table 1. The chemical composition of untreated fibers was 41.96 ± 1.82% cellulose, 41.14 ± 1.140 % hemicelluloses, 10.40 ± 1.32% lignin, and 6.50 ± 0.15% extractive, whereas for treated fibers, it was 70.20 ± 4.77% cellulose, 14.50 ± 0.50% hemicellulose, 13.10 ± 2.26% lignin, and 2.50 ± 0.23% extractive. After alkali treatment, the hemicellulose content of sisal fibers was reduced from 41.14 ± 1.14% to 14.50 ± 0.50% as hemicellulose is much more sensitive to the action of sodium hydroxide than lignin and cellulose [3]. The % of cellulose and lignin were increased after alkali treatment. Fibers with higher degree of polymerization, higher cellulosic content, and a lower microfibrile angle exhibit higher tensile strength and modulus [16, 18]. So, treating natural fibers with NaOH increases cellulosic content and enhances the roughness of the fiber which improves the fiber mechanical properties.

Scanning electron microscopy is an excellent technique to study surface morphology of materials [19, 20]. SEM images of untreated and alkali-treated sisal fibers are shown in Figure 2. Figure 2(a) is the SEM images of untreated sisal fiber showing impurities such as wax and extractive substances accumulated on the surface. These impurities may include lots of impurities and fibrils bound together by hemicellulose on the surface.

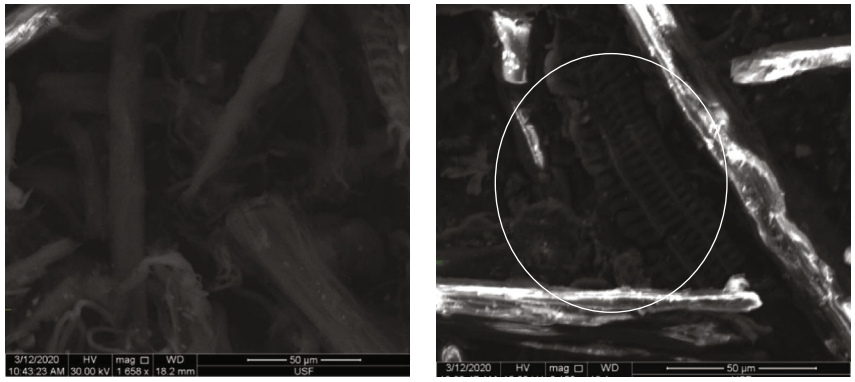

(a) (b)

Figure 2: SEM images of sisal fibers: (a) untreated (USF) and (b) treated (TSF).

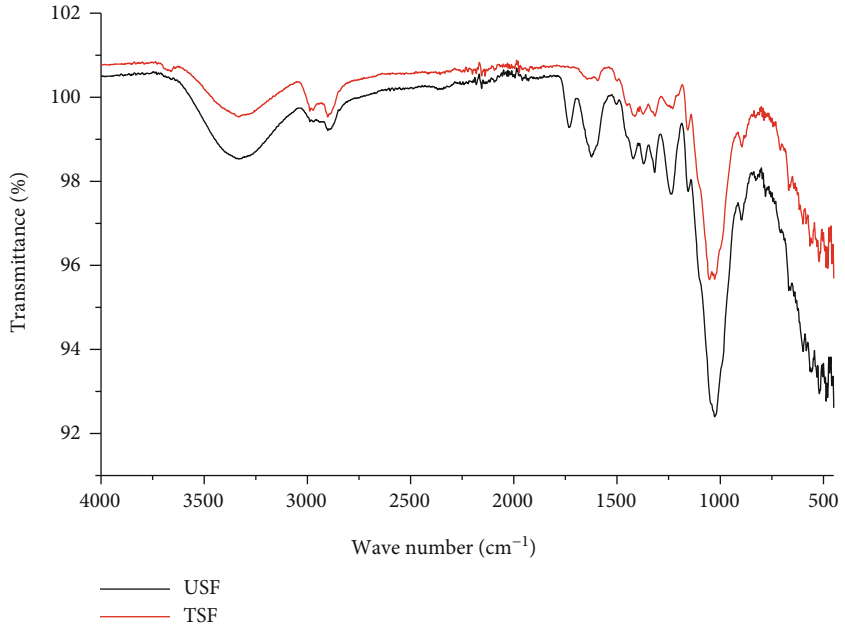

Figure 3: FTIR spectra of untreated and treated sisal fibers.

Alkali-treated fibers show relatively clean, and roughness surface (Figure 2(b)) is clearly seen in the circled area. This rough surface might be created due to the removal of impurities from the fiber. Considerable differences are observed on fiber morphology of untreated (Figure 2(a)) and treated (Figure 2(b)) fibers. The roughened surface may improve the intrusion of matrix to the fiber and the interfacial bonding when sisal fibers mix with matrix during composites preparation.

Untreated and treated sisal fibers were analyzed by FTIR spectrometer to study the chemical constituents on fiber surface. Figure 3 shows the FTIR spectra of the untreated and alkali-treated sisal fibers. The broad intense absorption band in the range of 3400-3300 cm^{-1} is due to O-H stretching vibrations of hydroxyl (OH) groups, present in the fiber [21].

The FTIR spectrum of alkali-treated fiber showed a decrease in intensity of the broad absorption around 3400-3300 cm^{-1} due to the removal of hydroxyl containing constituents of the fiber. A small peak absorption bands at 2950 and 2800 cm^{-1} correspond to the C-H stretching [5]. The absorption band at 1625 and 1725 cm^{-1} in the untreated fibers was assigned to the carbonyl groups (C=O) due to the presence of acetyl ester and carbonyl of aldehyde groups of hemicellulose and lignin [5, 21]. The intensity of this band is considerably decreased in the alkali-treated fiber due to the partial removal of the hemicellulose component. The sharp intense absorption band at 1367 cm^{-1} corresponds to the C-H asymmetric deformation of cellulose [21]. The absorption bands at 1050 and 1030 cm^{-1} correspond to C-O-C stretching in cellulose and hemicelluloses. According to [21, 22], the bands in the range of 1190 to 950 cm^{-1} can be attributed to the C-O and C-H vibrations that are derived from aliphatic -CH_2 or phenol -OH bonds. The slight decrease in intensity at this region confirms the removal of hydroxyl groups while treating the fiber with sodium hydroxide. The FTIR analysis revealed the existence of chemical components (cellulose,

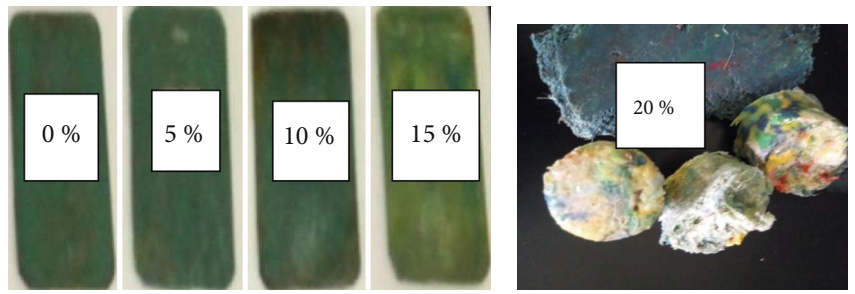

(a) (b)

Figure 4: Sisal fiber-reinforced polypropylene composite: (a) 0-15% fiber content and (b) 20% fiber content.

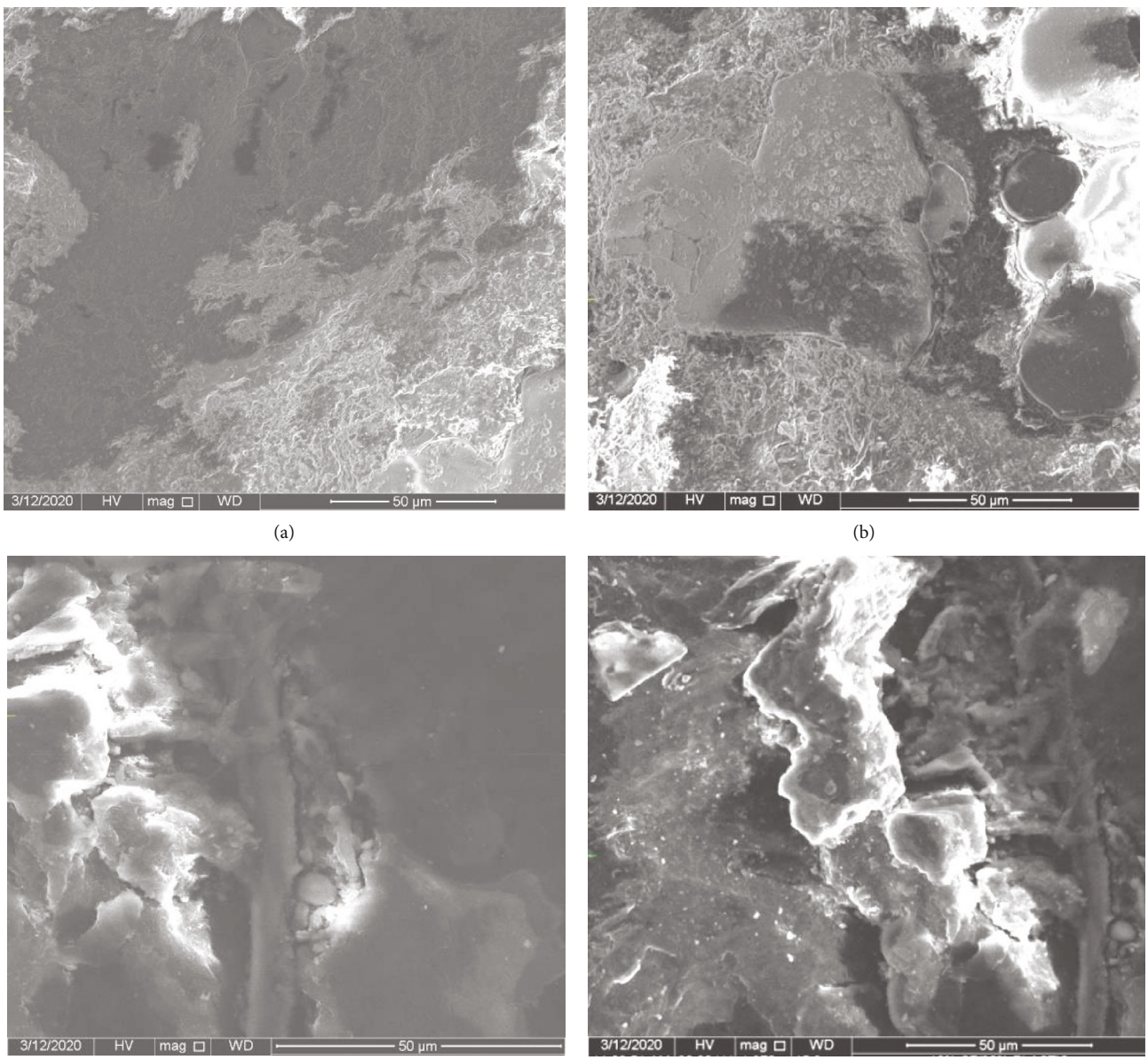

(a) (b)

(c) (d)

Figure 5: SEM images of composite (a) 0%, (b) 5%, (c) 10%, and (d) 15% fiber loading.

hemicellulose, and lignin) based on their functional groups observed in the spectra of sisal fibers and confirmed the reduction of the hemicellulose content by alkali treatment.

3.3. Composite Preparation with Different Fiber Loading. The composites were prepared with 0, 5, 10, 15, and 20% sisal fiber content in injection molding extruder (Thermo Forming Center 911). At low fiber loading 5% and 10%, the matrix was dominant as it was observed visually in Figure 4(a). A composite from 20% fiber was not good to be included for further experiment as shown in Figure 4(b) which can be justified by the limitation of the molding machine to mix the substrates [23], and it was difficult to remove the composite from the machine. However, the composite with 15% sisal fiber loading shows good surface features which is comparable with 5% and 10% fiber loadings.

3.3.1. Characterization of Composites Using SEM. The fiber and matrix adhesion of the composites was examined by SEM at 10 kv operating voltage. The SEM image of the prepared composite is used to study the nature of adhesion between the reinforcing fiber and the matrix. The SEM images of composites with different sisal fiber loading are shown in Figure 5. Figure 5(a) represents a composite with 0% fiber loading shows doughy and smooth surface feature. Figure 5(b) is the SEM image of the composite with 5% fiber which shows some roughness as compared to the pure matrix material (Figure 5(a)). Figure 5(c) shows SEM image of the composite material with 10% fiber. As it is seen, the surface roughness increases as fiber loading increases, and there are agglomerates and void spaces as compared to Figure 5(b). The image of the biocomposite with 10% fiber shows boundaries and nonuniformity on the surface. The area of the voids in Figure 5(c) is comparatively small as compared to the composite prepared with 15% fiber (Figure 5(d)). More nonuniformity, agglomeration, and roughness are observed in Figure 5(d) as compared to all others. Based on the observed results, it is possible to conclude that as the fiber content increases, surface roughness and nonuniformity increases [24]. This increases intrusion of matrix into the fiber and increases adhesion property of the substrates up to a certain extent. However, as the percentage of fiber increases, it may have side effects on properties of composites like water absorbing properties and facilitate decomposition of the composite.

3.4. Biodegradation of the Composite. Reinforcing plastic material with natural fibers is important to recycle plastic wastes and reduce environmental pollution as well as to produce partially degradable composite [17]. The degradability of the prepared composite materials was studied and the experimental result revealed partial biodegradability of composites. The percentage weight loss of samples increases as the percentage of sisal fiber increases in composites (Figure 6). The percentage weight loss of composites with 0, 5, 10, and 15% fiber loading is found to be 0.11, 4.62, 7.15, and 10.97%, respectively. This experimental result is consistent with the information obtained from previous characterization results like surface features of the composites with fiber loading. As the surface roughness of the composite increases, its water absorbing and holding potential increases; as a result, degradation increases.

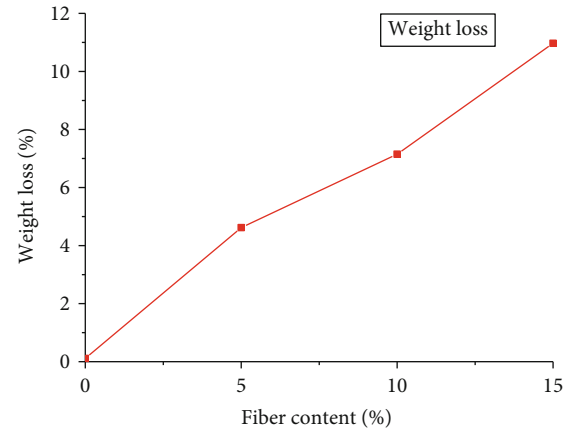

Figure 6: Percentage weight loss of the composites with different fiber loading.

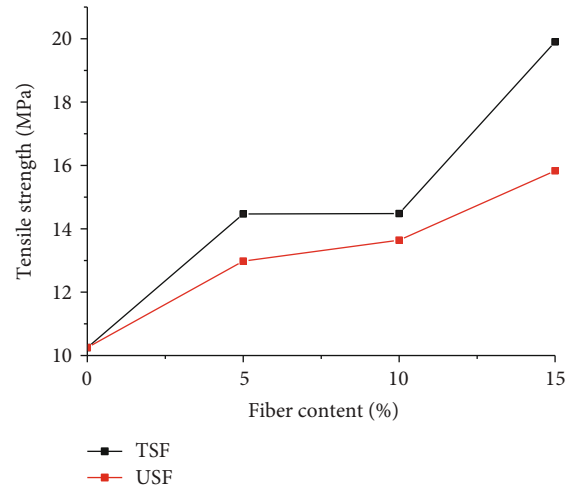

Figure 7: Tensile strength of composites from treated and untreated sisal fiber.

3.5. Mechanical Properties of the Composite

3.5.1. Effects of Fiber Treatment and Fiber Loading on Tensile Strength of the Composite. Tensile strength of composites from treated sisal fiber was 10.25 ± 0.50, 14.47 ± 0.20, 14.48 ± 0.12, and 19.90 ± 0.86 MPa for 0, 5, 10, and 15% fiber content, respectively, and the tensile strength of the composites from untreated sisal fiber was found to be 12.98 ± 0.20, 13.64 ± 1.73, and 15.83 ± 2.00 MPa for 5, 10, and 15% fiber content, respectively. With similar fiber loading, biocomposites from treated sisal fiber show relatively high strength than composites from untreated sisal fiber. This might be justified by the surface chemistry of the fiber before and after treatment which affects the interfacial adhesion of fiber and matrix. The chemical treatment of the fiber improves its adhesion property with the matrix by destroying hemicellulose and lignin which are present in natural fibers [25, 26]. When the fiber is treated, its hydrophilic nature of the fiber

Table 2: Comparison with previous works on tensile properties of natural fiber composites.

Matrix	Fiber	Fabrication method	Fiber/matrix ratio (%)	Tensile strength (MPa)	Reference
Waste PP	Sisal	Injection molding	5/95	14.47	This study
			10/90	14.48	
			15/85	19.9	
PP	Sisal	Injection molding	15/85	12.168	[27]
			20/80	20.14	
			25/75	14.11	
Polyester	Banana	Hand lay-up	10/90	11.03	[36]
			20/80	11.05	
			30/70	12.45	
Polyester resin	Jute	Hand lay-up	10/90	24.096	[28]
			15/85	20.12	
PE	Sisal	Injection molding	5/95	17.5	[12]
			10/90	18.3	
PP	Sisal	Hand lay-up	50/50	30	[37]
			40/60	40	
PP	Sisal	Injection molding	20/80	27.296	[38]
			30/70	26	
PE	Sisal	Injection molding	30/70	34.27	[29]
PE	Sisal	Injection molding	5/95	20	[38]
			10/90	21	
			30/70	31.12	

decrease and surface roughness of the fiber increases. These surface features increase the adhesion property of the fiber with the matrix. Hence, the increase in tensile strength of composites from treated fibers is resulted due to the removal of hemicellulose, lignin, and pectin that have the hydrophilic nature. Additionally, chemical treatment creates rough surfaces on fiber surfaces; as a result, it increases intrusion of the matrix into fibers.

The second factor that affects the tensile strength is the percentage of reinforcing fiber with the matrix. As it is displayed in Figure 7, tensile strength of composites increases as the fiber loading increase for both treated and untreated fibers. The specimen that has 0% of fiber loading resulted low tensile strength, 10.25 ± 0.50 MPa, but the tensile strength of the composites increased with increasing reinforcing fiber content. The peak strength of untreated sisal fiber composite were 12.98 ± 0.20, 13.64 ± 1.73, and 15.83 ± 2.00 MPa for 5, 10, and 15% fiber content, respectively, whereas the peak strength of composite from treated sisal fiber $14.47 \pm .0200$, 14.48 ± 0.12, and 19.90 ± 0.86 MPa for 5%, 10%, and 15% fiber content, respectively.

The tensile strength of the new composite is similar with more previously reported works as it is seen in Table 2. The tensile strength of the new material is similar with [12, 27–29] reported for composites with 15/85 fiber/matrix ratio.

3.6. Effect of Fiber Treatment and Fiber Loading on Elongation of Composites. The result of elongation of biocomposites from treated fiber was found to be 3.36 ± 0.03, 4.68 ± 0.26, and 3.40 ± 0.02% with fiber loading of 5, 10, and 15%, respectively,

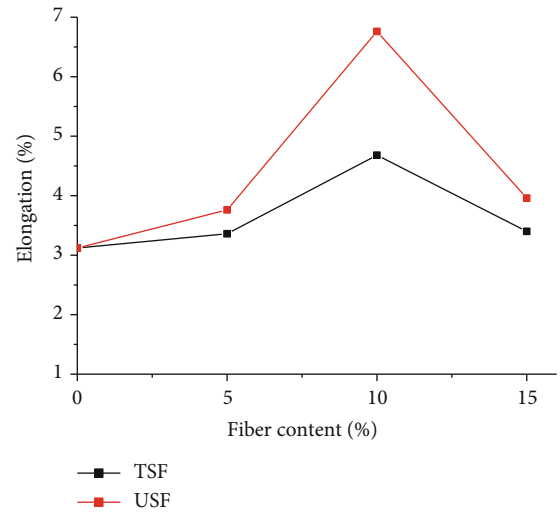

Figure 8: Elongation of composites from treated and untreated sisal fiber.

while for biocomposites from untreated fiber resulted 3.76 ± 0.17, 6.76 ± 0.02, and 3.96 ± 0.02% for fibber loading 5, 10, and 15%, respectively. The elongation of the biocomposites made from untreated sisal fibers (USFC) is somewhat higher than composites from treated fibers (TSFC). The lower % elongation at break for the alkali-treated sisal fiber composites might be resulted because of the removal of the extractive and pectin having elastic properties in sisal fibers [16]. The other factor that affects elongation is the contents of fibers in the

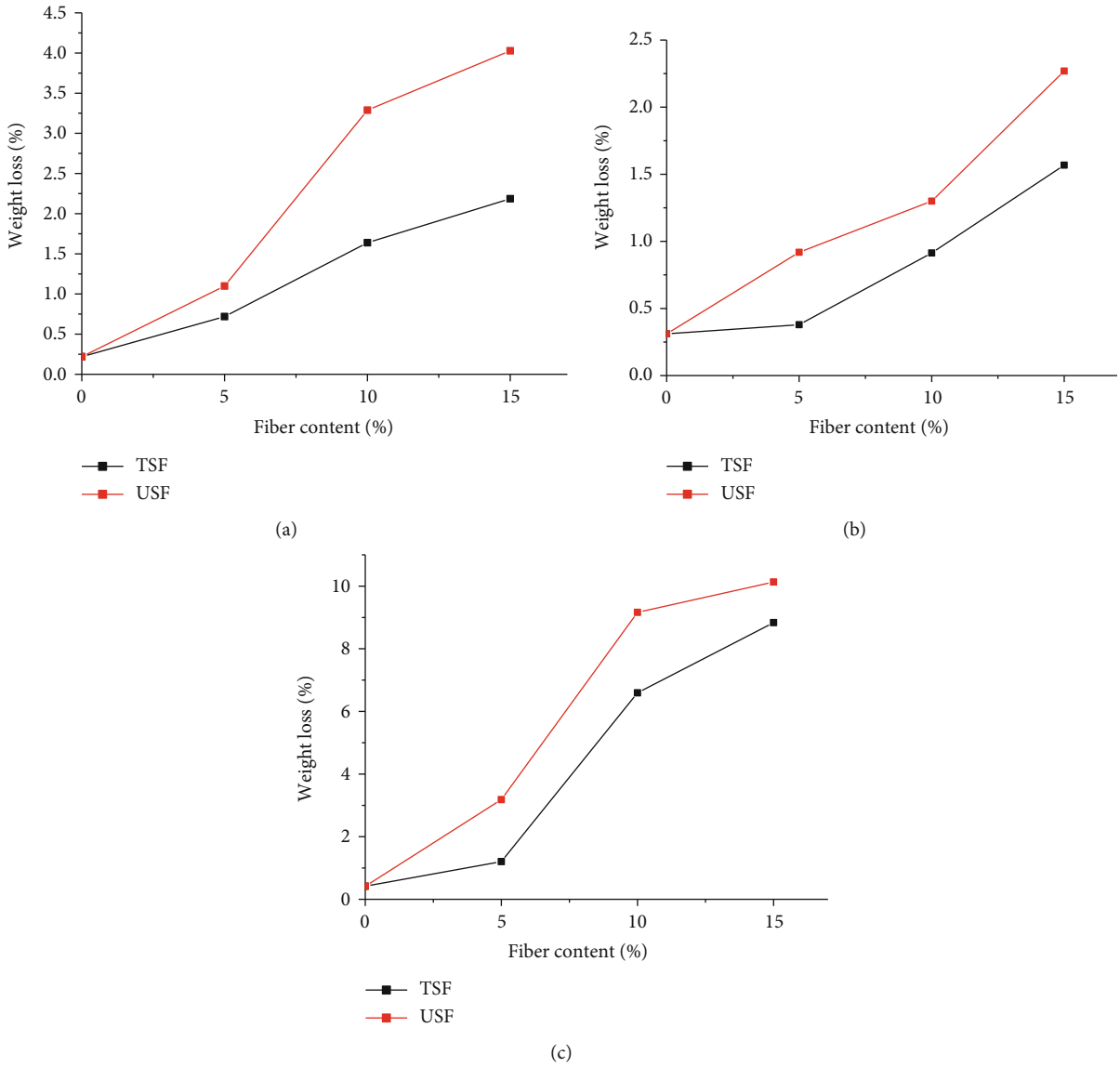

Figure 9: Percentage weight loss of composites in (a) 30% NaOH, (b) 30% HCl, and (c) 30% H_2SO_4.

composite. Biocomposites with 10% of fiber loading for both treated and untreated sisal fibers show maximum elasticity as shown in Figure 8. Elongation of biocomposites with 15% fiber loading decreased due to the decrease in ductility of the composites which can be due to the brittleness nature of the fiber. Similar observations were also reported previously [16, 29].

3.7. Chemical Resistance Test

3.7.1. Composite Resistance to 30% NaOH, 30% HCl, and 30% H_2SO_4 Solutions. The effect of treatment of fiber and fiber loading on resistance to sodium hydroxide (NaOH) is displayed in Figure 9(a). Weight loss (%) from untreated sisal fiber composite was found to be 0.219, 1.099, 3.289, and 4.027 for 0%, 5%, 10%, and 15% fiber loading, respectively, whereas weight loss (%) from treated sisal fiber composites was 0.219, 0.719, 1.638, and 2.186 for fiber loading of 0, 5, 10, and 15%, respectively. For both treated and untreated fiber, as the fiber content increased, the weight loss also increased indicating the susceptibility of the composites to NaOH with an increase of fiber content. In addition to fiber loading, fiber treatments also have significant effect on the weight loss. Compared to untreated composites, treated composites showed lower weight loss which might be due to the susceptibility of hemicellulose and lignin for reaction in composites from untreated fibers. When composites treated with hydrochloric acid, the fiber loading and fiber treatment resulted a significant effect on the percentage weight loss (Figure 9(b)). The weight loss of composites from untreated fiber was 0.919, 1.300, and 2.269% for fiber loading of 5, 10, and 15%, respectively. The maximum weight loss (2.269%) was observed for the composite with 15% of untreated fiber loading. This can be justified by the chemical nature of treated and untreated fibers. The degradation effect of H_2SO_4 on composites from treatment and untreated fibers is displayed in Figure 9(c). The weight losses of composites

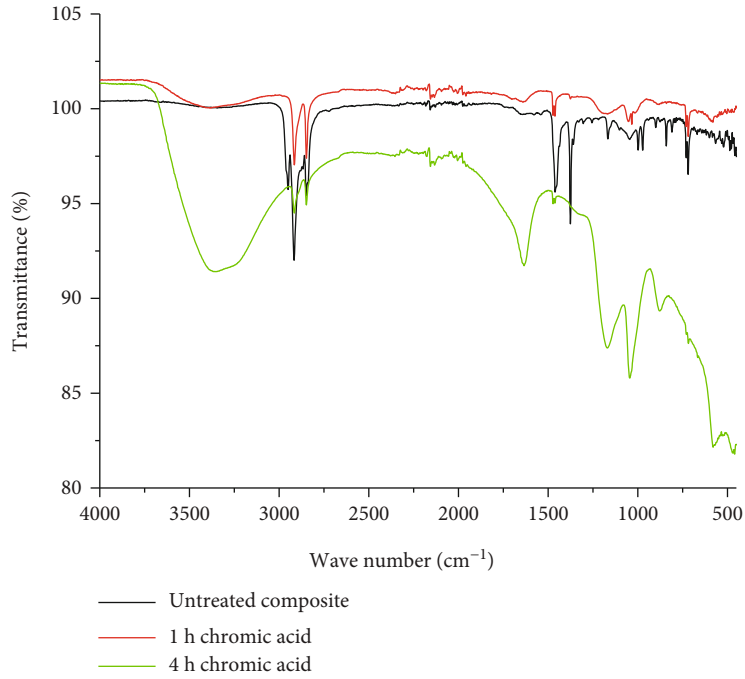

Figure 10: FTIR spectra of untreated and chromic acid etched composite for 1 and 4 h.

from untreated fiber were 0.419, 3.183, 9.163, and 10.131% for fiber loadings of 0, 5, 10, and 15%, respectively. For similar fiber loading, low weight loss was observed for composites from treated sisal fiber as compared to composites from untreated sisal fiber. The weight losses of composites from treated fiber are 1.203%, 6.592%, and 8.834% for fiber content of 5, 10, and 15%, respectively. The chemical resistance of composites from treated fiber had good resistance for chemicals than composites from untreated fiber which might be justified by good bonding nature of treated fibers with the matrix.

Based on all above physicochemical evaluation results, biodegradability, tensile strength, elongation, and resistance to chemicals, a composite with 15% treated fiber content was considered as optimum product in this experiment. As a result, a composite with similar fiber content (treated) was considered for surface modification.

3.8. Surface Modification and Characterization. In addition to surface roughness, surface chemistry modification with low surface energy is important to enhance superhydrophobicity [30]. FTIR is the most powerful tool to identify the types of chemical bonds and functional groups present on material surfaces. In this study, FTIR spectrum was obtained to determine the change in functional groups due to surface etching. Figure 10 shows the FTIR spectra of composites before chromic acid treatment, and after 1 h and 4 h chromic acid treatment. The untreated composite shows a different spectrum from the other two samples which are etched with chromic acid for 1 h and 4 h. A sample treated for 1 h shows little chemical modification as compared to untreated one. However, after 4 h treatment of the sample, a broad band around 3341-3235 cm^{-1} refers to hydroxyl groups in carboxylic acids that indicate oxidative reactions. This result provides a supportive evidence for change in chemical composition of the surface. The other new peak at 1625.91 cm^{-1} is assigned to C=O due to further oxidation of C-OH to carboxylic acid group (COOH). Time of aching is an important factor for the type of functional groups on the surface; as the time of etching increases, C-H becomes oxidized to C-OH and then further oxided to -COOH [14]. A weak peak at 1463 cm^{-1} for ununtreated composite shows the presence of C-H, while after treatment, the intensity of the peak was decreased as a result of oxidation of C-H to C-OH and -COOH.

3.9. SEM Analysis of Untreated and Chromic Treated Composite Surfaces. In order to achieve superhydrophobicity, surfaces need to possess hierarchical micro- and nanoroughness and low surface energy at the same time. Rough surface increases the solid liquid interface and also increases air trapped between the surface and liquid droplet [31]. The surface structure of the biocomposite (before and after etching) was characterized by SEM as shown in Figure 11. The SEM image of untreated composite shows smooth surface (Figure 11(a)), and the SEM image of chromic acid-treated sample (1 hr) shows chain scission and destruction of amorphous parts without clear structure at a given magnification (Figure 11(b)). As the chromic acid treatment time increased to 4 hrs, the roughness of the sample increased as shown in Figure 11(c). This etching process changes not only the surface morphology but also the chemical composition of the surface.

The composite material which was etched by chromic acid was treated again with low surface energy chemical, stearic acid, and then, the composite was analyzed using FTIR. After stearic acid treatment, the FTIR spectrum (Figure 12)

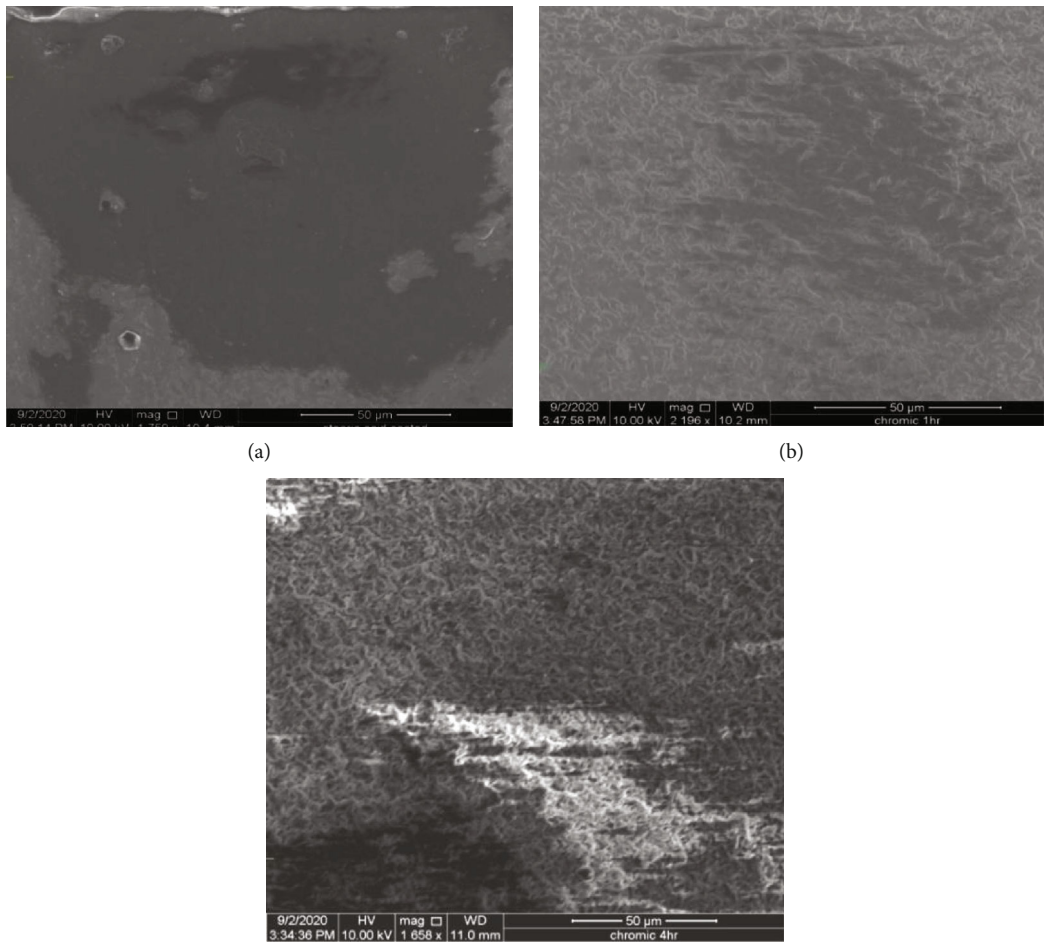

(a) (b)

(c)

Figure 11: SEM images of a composite (a) before chromic acid etching and (b) after etching for 1 h and (c) for 4 h.

shows the disappearance of a strong broad band at about 3377 cm^{-1}. This confirms the condensation reaction of OH groups in carboxylic acid with stearic acid (esterification). Additionally, the absorption bands around 1625 cm^{-1} was disappeared which is an indication of reaction of carbonyl groups of the composite surface with stearic acid, and the new peak at 1688 cm^{-1} confirms the presence of C=O stretching for carboxyl groups in esters (Scheme 1).

3.10. Wet Ability of Surface Modified and Unmodified Composites. Commonly, wet ability is determined by the value of the contact angle (CA), which is the angle formed between the tangent to the liquid and the materials surface at the interface between solid and liquid phases. Surface wet ability is understood as a material ability to retain water on its surface as a result of the presence of mist, rain, or dew. In this work, the composite surface before any modification shows a wet able (hydrophilic) character as shown in Figure 13(a) with droplets disperse over the surface of the composite.

However, the surface hydrophobicity of the composite was enhanced through etching the composite surface with chromic acid (Figure 13(b)) and to modify the surface composition resulting a poorly wet able (hydrophobic) composite surface. Further treatment of the etched surface with stearic acid provided the characteristic of superhydrophobicity by forming perfect ball like droplets (Figure 13(c)). The gained superhydrophobic characteristic of the composite surface was further confirmed by evaluating its self-cleaning property.

3.11. Self-Cleaning Properties of Modified and Unmodified Composite Materials. Self-cleaning properties is another method to determine whether the material surface is hydrophilic, hydrophobic, or superhydrophobic. For a surface to be classified as both superhydrophobic and self-cleaning, it must have a contact angle greater than 150° and a contact angle hysteresis (ΘH) less than 5° [32]. Contact angle hysteresis is the difference between the advancing (ΘADV) and the receding (ΘREC) contact angles of a moving droplet over a solid surface [33]. Both the contact angle and contact angle hysteresis measure the surface wet ability and self-cleaning properties. If the surface show self-cleaning properties, it has small contact angle hysteresis, and the contact angle is larger than 150° which means the surface is superhydrophobic. If the hysteresis is large and the contact angle is less than 150°, water droplets would not roll off the surface carrying contaminants with them; instead, they would slide slowly off the surface smearing any dirt particles/contaminants along the way as shown on unmodified composite surface

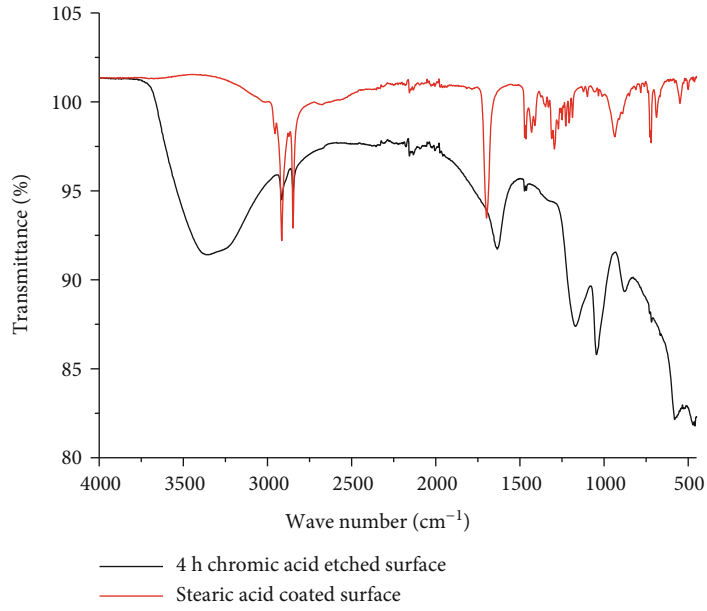

Figure 12: FTIR spectrum of composite material before and after surface modification.

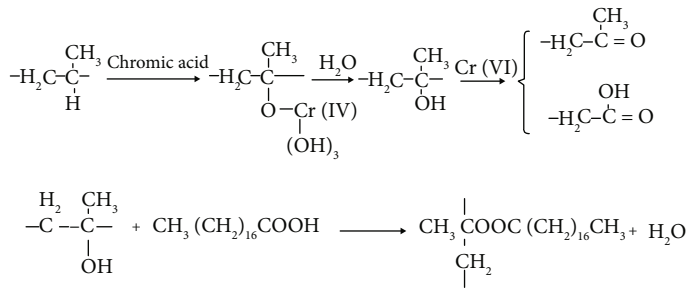

Scheme 1

(a) (b) (c)

Figure 13: Water droplets on composite material (a) before surface modification, (b) chromic acid etched, and (c) stearic acid-modified surface.

in Figure 14(a). However, the modified surface showed self-cleaning properties by collecting dirt and contaminant particles with water droplet rolling over the surface Figure 14(b). The superhydrophobic surface with self-cleaning property was achieved by a combined effect of surface roughness resulted by etching the surface with chromic acid and through surface treatment with low energy chemical (stearic acid).

3.12. Water Absorption Capacity of Composites before and after Surface Modification. Increasing natural fiber content in the composite materials is desirable because it assists in

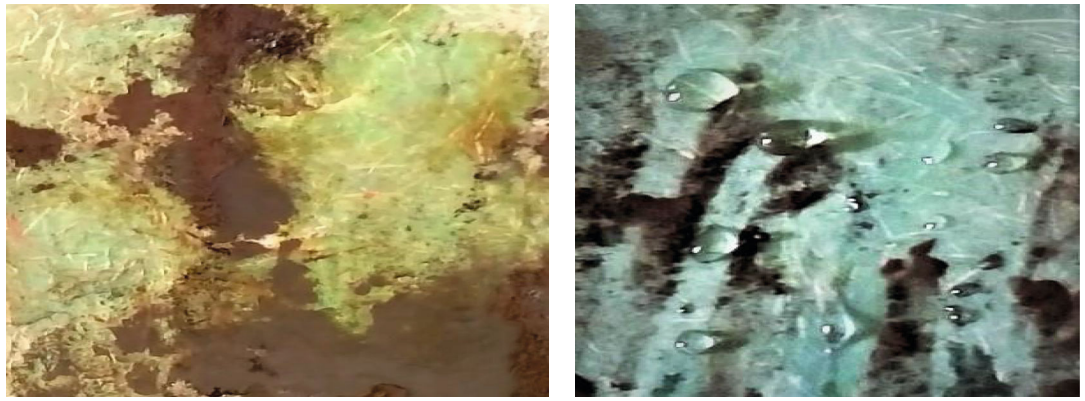

(a) (b)

Figure 14: Self-cleaning properties of composite material (a) before surface modification and (b) after surface modification.

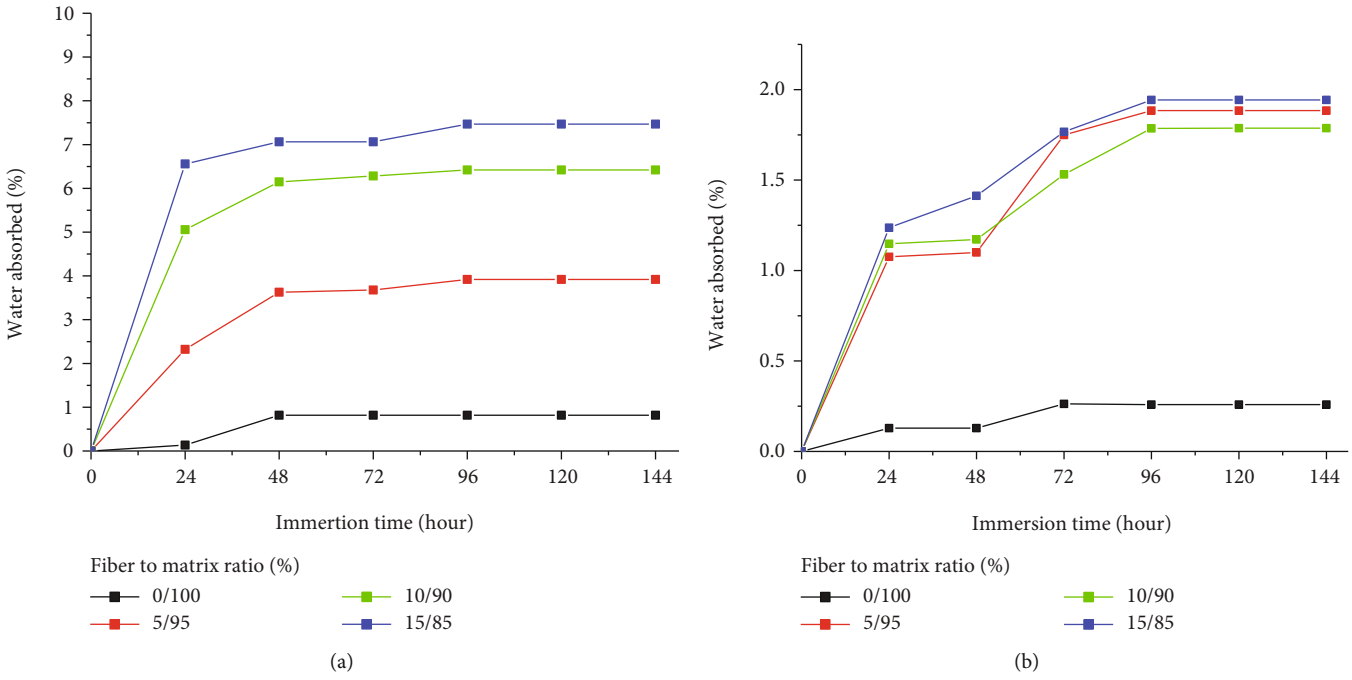

Figure 15: Water absorption percentage (%) of (a) unmodified composites and (b) modified composite at different time intervals.

reducing the cost, protecting the environment by increasing biodegradability and increasing the mechanical properties of composite materials [34]. However, the water absorption capacity of natural fiber reduces the mechanical properties of composites. The water absorption of composites can be reduced by treatment of natural fibers and by modifying the surface of composites [35].

In this experiment, the moisture absorption property of the modified and unmodified composites was evaluated by immersing specimens with known mass and was in water for 144 h at room temperature, and the weight of the specimen was recorded in every 24 h intervals. The water absorption property of both modified and unmodified composites was increased with the fiber content. The water absorption curves of different composite samples of both unmodified and modified are presented in Figure 15. The plot shows that water absorption of composites was increased with immersion time until equilibrium condition was reached (at about 96 hours) in both cases. For unmodified composite, the maximum water absorption was 0.818, 3.919, 6.421, and 7.467% for 0, 5, 10, and 15 wt% fiber contents, respectively (Figure 15(a)). As the sisal fiber contents increase, water absorption property increases which might be due to the proportionality of -OH groups that enhance hydropholicity. At the same time, the surface roughness and porosity increases water holding capacity of the composites. After 96 hrs immersion time, the maximum water absorption capacity of the unmodified composite with 15 wt% sisal fiber was 7.467 wt% while the surface modified composite with same fiber loading was 1.943 wt Figure 15(b). Our result is consistent with previously reported theories: water absorption behavior of natural fiber composites is largely affected by

many factors such as the chemical and physical treatments of natural fibers, fiber content, immersion time, and modification of composite surfaces [13]. The water absorption of the surface modified composite is 0.259, 1.884, 1.786, and 1.943% for 0, 5, 10, and 15 wt% sisal fiber loadings, respectively (Figure 15(b)) at 96 hrs which is significantly low as compared to unmodified composites. After immersion time of about 52 hrs, the modified composite with 10% fiber loading shows lower water absorption as compared to the composite with 5% fiber loading. This might be due to an experimental error originated from nonuniformity of surface features on composites with 5% fiber content like surface roughness originated during material preparation or surface modification.

The experimental results clearly show the effect of superhydrophobicity on water absorption property of the composites. The low water absorption property of the composite helps to decrease its degradation and increase service life.

4. Conclusions

In this study, the biocomposite material with superhydrophobic surface is prepared successfully using clearly defined procedures. The composite material is prepared by reinforcing recycled polypropylene with sisal fiber. The sisal fiber was treated with NaOH to decrease its hydrophilic property and to improve the compatibility of the fiber with polyethylene. Composites were prepared using different percentage of sisal fiber, and the mechanical and physicochemical properties were evaluated to obtain the optimum ratio of fiber and polyethylene. The composite with 15% fiber content was taken as optimum composition, and it was further treated with chromic acid and stearic acid to modify the surface properties. Surface modification was done by treating the composite with chromic acid, to get rough surface and to introduce new chemical groups followed by the surface treatment with low energy chemical, stearic acid. The analytical results of SEM image and FTIR spectra revealed the real change of surface morphology and chemical composition during chromic acid etching and stearic acid treatment. Finally, the prepared composite showed self-cleaning property which is a characteristic property of superhydrophobicity. And this was supported by low water absorption property of the composite as compared to with unmodified ones. The final product is supposed to be suitable for those application areas working with moisture susceptible products.

Data Availability

The video and figure used to support the findings of this study are included within the supplementary information file(s).

Conflicts of Interest

The authors declare that there is no conflict of interest regarding the publication of this paper.

Acknowledgments

We would like to acknowledge Department of Industrial Chemistry and Nanotechnology Center of Excellence at Addis Ababa Science and Technology University. This research was supported by Addis Ababa Science and Technology University.

Supplementary Materials

Self-cleaning and wet ability properties of unmodified and modified composite surfaces were tested, and images and videos were recorded as attached herewith. *(Supplementary Materials)*

References

[1] B. Worm, H. K. Lotze, I. Jubinville, C. Wilcox, and J. Jambeck, "Plastic as a persistent marine pollutant," *Annual Review of Environment and Resources*, vol. 42, no. 1, pp. 1–26, 2017.

[2] J. Manzoor, M. Sharma, I. R. Sofi, and A. A. Dar, "Plastic waste environmental and human health impacts," in *Handbook of Research on Environmental and Human Health Impacts of Plastic Pollution*, IGI Global, 2020.

[3] N. Dinh Vu, H. Thi Tran, and T. Duy Nguyen, "Characterization of polypropylene green composites reinforced by cellulose fibers extracted from rice straw," *International Journal of Polymer Science*, vol. 2018, 10 pages, 2018.

[4] J. W. Kaczmar, J. Pach, and R. Kozlowski, "Use of natural fibers as fillers for polymer composites," *International Polymer Science and Technology*, vol. 33, no. 11, pp. 722–726, 2006.

[5] N. Ramli, N. Mazlan, Y. Ando et al., "Natural fiber for green technology in automotive industry: a brief review," *IOP Conference Series: Materials Science and Engineering*, vol. 368, article 012012, 2018.

[6] A. Cantalino, E. A. Torres, and M. S. Silva, "Sustainability of sisal cultivation in Brazil using co-products and wastes," *Journal of Agricultural Science*, vol. 7, no. 7, pp. 64–72, 2015.

[7] P. N. Khanam and M. A. A. AlMaadeed, "Processing and characterization of polyethylene-based composites," *Advanced Manufacturing: Polymer & Composites Science*, vol. 1, no. 2, pp. 63–79, 2015.

[8] M. Kebede, *Fabrication and Mechanical Property Characterization of Sisal Fiber Reinforced Epoxy Resin Composite Material for Automotive Body Application [M.S. thesis]*, Addis Ababa University, 2015.

[9] K. C. Hung, H. Yeh, T. C. Yang, T. L. Wu, J. W. Xu, and J. H. Wu, "Characterization of wood-plastic composites made with different lignocellulosic materials that vary in their morphology, chemical composition and thermal stability," *Polymers*, vol. 9, no. 12, p. 726, 2017.

[10] A. G. Gerezgiher, H. A. Bsrat, A. Simon, and T. Szabó, "Development and characterization of sisal fiber reinforced polypropylene composite materials," *International Journal of Engineering and Management Sciences*, vol. 4, no. 1, pp. 348–358, 2019.

[11] K. O. Reddy, B. Ashok, K. R. N. Reddy, Y. E. Feng, J. Zhang, and A. V. Rajulu, "Extraction and characterization of novel lignocellulosic fibers from Thespesia lampas plant," *International Journal of Polymer Analysis and Characterization*, vol. 19, no. 1, pp. 48–61, 2014.

[12] S. L. Favaro, T. A. Ganzerli, A. G. V. de Carvalho Neto, O. R. R. F. Da Silva, and E. Radovanovic, "Chemical, morphological and mechanical analysis of sisal fiber-reinforced recycled high-density polyethylene composites," *Express Polymer Letters*, vol. 4, no. 8, pp. 465–473, 2010.

[13] N. Venkateshwaran, A. ElayaPerumal, and M. S. Jagatheeshwaran, "Effect of fiber length and fiber content on mechanical properties of banana fiber/epoxy composite," *Journal of Reinforced Plastics and Composites*, vol. 30, no. 19, pp. 1621–1627, 2011.

[14] A. M. Mansora, J. S. Lima, F. N. Anib, H. Hashima, and W. S. Hoa, "Characteristics of cellulose, hemicellulose and lignin of MD2 pineapple biomass," *Chemical Engineering*, vol. 72, pp. 79–84, 2019.

[15] H. Wang, S. Chen, and J. Zhang, "Surface treatment of LLDPE and LDPE blends by nitric acid, sulfuric acid, and chromic acid etching," *Colloid and Polymer Science*, vol. 287, no. 5, pp. 541–548, 2009.

[16] D. L. A. Abasiwie, *Mechanical Characterization of Biocomposites Fabricated from natural Coconut Fibre and Linear Low Density Polyethylene*, Msc. Thesis, Kwame Nkrumah University of Science and Technology, Kumasi Ghana, 2015.

[17] A. Ali, K. Shaker, Y. Nawab et al., "Hydrophobic treatment of natural fibers and their composites—a review," *Journal of Industrial Textiles*, vol. 47, no. 8, pp. 2153–2183, 2018.

[18] S. Taj, M. A. Munawar, and S. Khan, "Natural fiber-reinforced polymer composites," *Proceedings-Pakistan Academy of Sciences*, vol. 44, no. 2, pp. 129–144, 2007.

[19] S. K. Sethi and G. Manik, "Recent progress in super hydrophobic/hydrophilic self-cleaning surfaces for various industrial applications: a review," *Polymer-Plastics Technology and Engineering*, vol. 57, no. 18, pp. 1932–1952, 2018.

[20] P. Li, *Properties of Agave Fiber Reinforced Thermoplastic Composites*, Msc. Thesis, Iowa State University Ames, Iowa, 2017.

[21] I. Kubovský, D. Kačíková, and F. Kačík, "Structural changes of oak wood main components caused by thermal modification," *Polymers*, vol. 12, no. 2, p. 485, 2020.

[22] P. K. Adapa, C. Karunakaran, L. G. Tabil, and G. J. Schoenau, "Potential applications of infrared and Raman spectromicroscopy for agricultural biomass," *Agricultural Engineering International: CIGR Journal*, vol. 11, 2009.

[23] F. K. Liew, S. Hamdan, M. R. Rahman, and M. Rusop, "Thermomechanical properties of jute/bamboo cellulose composite and its hybrid composites: the effects of treatment and fiber loading," *Advances in Materials Science and Engineering*, vol. 2017, Article ID 8630749, 10 pages, 2017.

[24] B. Neher, M. A. Gafur, M. A. Al-Mansur, M. M. R. Bhuiyan, M. R. Qadir, and F. Ahmed, "Investigation of the surface morphology and structural characterization of palm fiber reinforced acrylonitrile butadiene styrene (PF-ABS) composites," *Materials Sciences and Applications*, vol. 5, no. 6, pp. 378–386, 2014.

[25] J. Naveen, M. Jawaid, P. Amuthakkannan, and M. Chandrasekar, "Mechanical and physical properties of sisal and hybrid sisal fiber-reinforced polymer composites," in *Mechanical and physical testing of biocomposites, fibre-reinforced composites and hybrid composites*, pp. 427–440, Woodhead Publishing, 2019.

[26] M. Z. Khan and S. K. Srivastava, "Development, characterization and application potential of bio-composites: a review," *Materials Science and Engineering*, vol. 404, no. 1, pp. 12–28, 2018.

[27] A. Francis, S. Rajaram, A. Mohanakrishnan, and B. Ashok, "Mechanical properties of sisal fibre reinforced polymer matrix composite," *Mechanics and Mechanical Engineering*, vol. 22, no. 1, pp. 295–300, 2020.

[28] E. A. Elbadry, M. S. Aly-Hassan, and H. Hamada, "Mechanical properties of natural jute fabric/jute mat fiber reinforced polymer matrix hybrid composites," *Advances in Mechanical Engineering*, vol. 4, 2012.

[29] U. Sudhakar, B. V. Suresh, and M. Raju Bahubalendruni, "A review on physical and chemical properties of natural fiber reinforced composite materials," *International journal of Science and Development Research*, vol. 3, pp. 160–172, 2018.

[30] J. Du, L. Zhang, J. Dong, Y. Li, C. Xu, and W. Gao, "Preparation of hydrophobic nylon fabric," *Journal of Engineered Fibers and Fabrics*, vol. 11, no. 1, article 155892501601100, 2016.

[31] Z. Wang, L. Shen, W. Jiang, M. Fan, D. Liu, and J. Zhao, "Superhydrophobic nickel coatings fabricated by scanning electro deposition on stainless steel formed by selective laser melting," *Surface and Coatings Technology*, vol. 377, article 1248, 2019.

[32] Y. Xiu, *Fabrication of surface micro- and nanostructures for superhydrophobic surfaces in electric and electronic applications*, PhD. Thesis, School of Chemical and Biomolecular Engineering, Georgia Institute of Technology, 2008.

[33] J. J. Victor, *Biology inspired nano-materials : superhydrophobic surface*, PhD. Thesis, Department of Materials Science and Engineering, University of Toronto, 2012.

[34] P. S. Kumar, C. U. Kiran, and K. P. Rao, "Effect of fiber surface treatments on mechanical properties of sisal fiber polymer composites–a review," *International Journal of Advanced Research in Science, Engineering and Technolology*, vol. 4, pp. 4411–4416, 2017.

[35] O. O. Daramola, O. S. Akintayo, T. A. Adewole, and H. K. Talabi, "Mechanical properties and water absorption behaviour of polyester/soil-retted Banana fibre (SRBF) composites," *Annals of the Faculty of Engineering Hunedoara*, vol. 15, no. 1, pp. 183–190, 2017.

[36] O. O. Daramola, A. A. Adediran, B. O. Adewuyi, and O. Adewole, "Mechanical properties and water absorption behaviour of treated pineapple leaf fibre reinforced polyester matrix composites," *Leonardo Journal of Sciences*, vol. 30, pp. 15–30, 2017.

[37] G. Bv, K. V. Krishna, M. H. Rather, and C. B. Mohan, *Sisal Fibre Reinforced Polypropylene Bio-Composites for Inherent Applications*, Institute of Scholars (InSc), 2019, http://www.insc.in.

[38] S. Somashekhar, G. C. Shanthakumar, and M. Nagamadhu, "Influence of fiber content and screw speed on the mechanical characterization of jute fiber reinforced polypropylene composite using Taguchi method," *Materials Today: Proceedings*, vol. 24, pp. 2366–2374, 2020.